Kodaikanal Obs. Bull. Ser. A (1979) **2**, 195-202

REFLECTION NEBULA IN THE FAR-ULTRAVIOLET

2. Silicate and Graphite Grains

G. A. SHAH and K. S. KRISHNA SWAMY*

ABSTRACT

Simple models of the reflection nebula in the form of homogeneous plane-parallel slab containing single scattering silicate and graphite grains taken one species at a time have been considered in view of the far-ultraviolet surface brightness observations obtained from the ANS satellite. The colour difference between the star and the nebula as well as the polarization of the nebular light in the far-ultraviolet have also been given.

Key words : reflection nebula—interstellar grains—far-ultraviolet colours and polarization

1. Introduction

As a sequel to the earlier work (Shah and Krishna Swamy, 1978, hereafter referred to as paper 1) on models of reflection nebula in the far ultraviolet using ice grains, we have investigated here the effects of silicate and graphite grains on the surface brightness, colour differences and polarization especially in view of the ANS satellite observations on surface brightness across the Merope reflection nebula.

In paper I, we showed that the ratio of the optical depths for small and large (classical) components of the grains in the nebula is much smaller than unity based on the assumption that the total surface area of small particles is two times larger than that of the larger particles. However, if one considers the small grains to be produced as a result of shattering of the larger grains, it appears to be more appropriate to guess that the total volume of the extremely small grains about equals that of the classical grains rather than the total surface area. Let a_1 and a_2 be the effective radii of the small and large categories of grains respectively. We assume both types of grains to be homogeneous spheres. If Q_1 and Q_2 are the corresponding extinction efficiencies, we derive analytically the volume ratio

$$f_v = \frac{V_1}{V_2} = \frac{n_{o1}}{n_{o2}}\left(\frac{a_1}{a_2}\right)^3 \qquad (1)$$

where V_1 = total volume of the small grains,

V_2 = total volume of the large grains,

and n_{o1}, n_{o2} are the corresponding number densities of the grains.

In deriving equation (1), we have assumed the Oort-Van de Hulst type of size distribution function in the form $n(a)\,da \sim (n_{o1}/a_1)\exp[-6(a/a_1)^3]\,da$. Note that the size parameter a_1 in the first bracket occurs because of proper normalization. The ratio of the optical depths τ_1 and τ_2 by the two categories of grains is then given by

$$\frac{\tau_1}{\tau_2} = f_v\left(\frac{a_2}{a_1}\right)\left(\frac{Q_1}{Q_2}\right) \qquad (2)$$

Assuming $f_v = 1$, $a_1 = 100\text{Å}$, $a_2 = 0.6\ \mu$m, and, as an illustration, choosing ice with typical refractive index $m = 1.33 - i\,0.05$ and $\lambda = 1500\text{Å}$, one obtains $\tau_1/\tau_2 \simeq 1/6$ on considering only the scattering optical depths or $\tau_1/\tau_2 \sim 1.3$ if both scattering and absorption are included. The total optical depth as explained in paper 1 is expected to be less than unity. This implies that single scattering on the classical grains is still an important factor in the phenomena of Merope reflection nebula. Furthermore, introduction of large absorptivity in the far-ultraviolet goes against the multiplicity of scattering because albedo would be reduced much below unity. Therefore, we have

* Tata Institute of Fundamental Research, Colaba, Bombay.

adopted the single scattering in the present work also.

It may be noted that volume equivalence between small and large grains would apply if the former are formed only by the shattering process. However, the mechanism of formation of the grains is still an open question. The choice of surface areas for comparison of optical depths as done in paper I has natural appeal because surface area of a grain is proportional to the geometrical cross-section, which in turn is related to the scattering cross-section, a quantity crucial for estimation of the optical depth. If extremely small grains are thought to form on the surface of the classical grains, the surface area seems to be all the more appropriate quantity. On the other hand, if the small grains form from the gas phase, the volume equivalence no longer holds.

2. The Computational Results from the Models

Following paper I, we assume single and independent scattering of light by grains within the nebula in the form of homogeneous plane-parallel slab. The three geometrical cases for star behind the nebula (SBN), star within the nebula (SWN) and star in front of the nebula (SFN) have been treated with the same values of geometric parameters given in Table 1 of paper I. The exception is to be found in Figure 3 where we have plotted a sample calculation for the distance of the star from the front surface of the nebula (H) equal to 0.05 pc, other quantities remaining the same. The necessary equations, notation, definitions and procedure are exactly as described in paper I. The only change in obtaining the present results is the consideration of enstatite silicate and graphite grains instead of ice grains. We have adopted the wavelength dependent refractive indices of graphite and silicate materials according to Philip and Taft (1962) and Huffman and Stapp (1971), respectively.

The abscissae in all the figures represent the offset angle ϕ in minutes of arc. The observational data (Andriesse *et al.* 1977) available only for the surface brightness of the Merope reflection nebula are denoted by dots in the Figures 1 to 8. It may be recalled that the far-ultraviolet bands designated U_1, U_2, U_3 and U_4 have ranges of wavelengths (Å) 2150-3200, 1550-3150, 1350-2300 and 1050-2300, respectively.

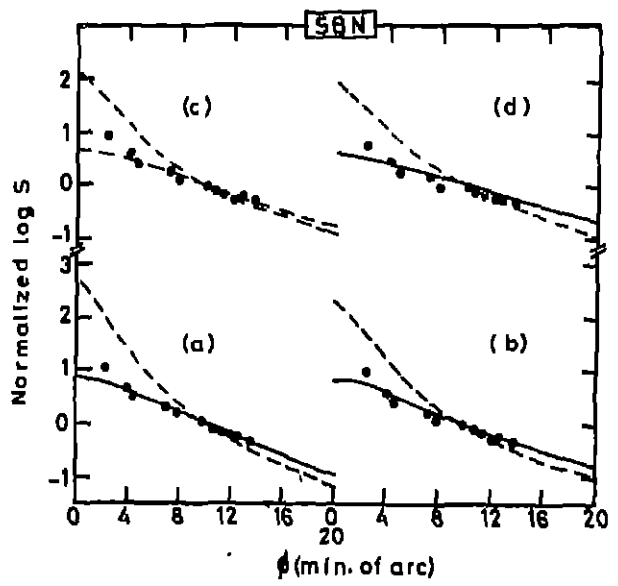

Fig. 1. The far-ultraviolet nebular surface brightness in arbitrary units but normalized such that log S (λ, s_0, $\phi = 10'$) = log S_{obs} ($\phi = 10'$) = 0 for the case of the star behind the nebula (SBN) and graphite grains. The sets (a), (b), (c) and (d) correspond to wavelengths $\lambda = 1550$Å, 1800Å, 2200Å and 2500Å, respectively. The graphite grains have size parameter $s_0 = 0.1$ μm for _____ and 0.4 μm for – – – –. The dots represent satellite observations.

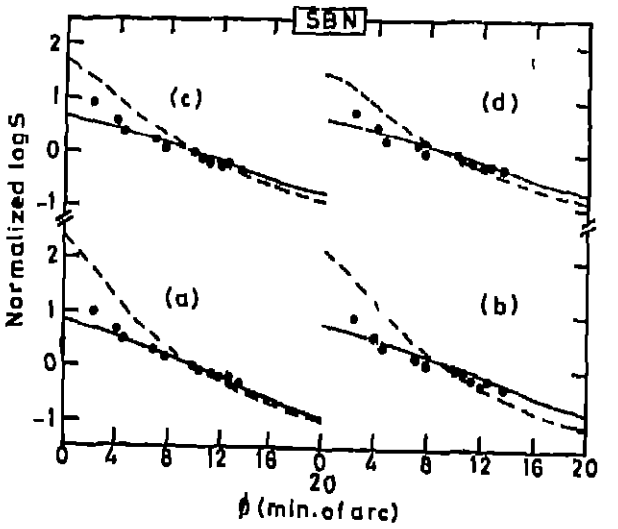

Fig. 2. The same as Figure 1, but for enstatite grains.

2.1 *Surface brightness*

The calculated results on surface brightness for the three geometrical cases SBN, SWN and SFN are shown in Figures (1,2), (3,4) and (5,6), respectively; here and subsequently the odd numbered figures are for graphite and the even numbered figures are for enstatite silicate. The surface brightness (S) of the

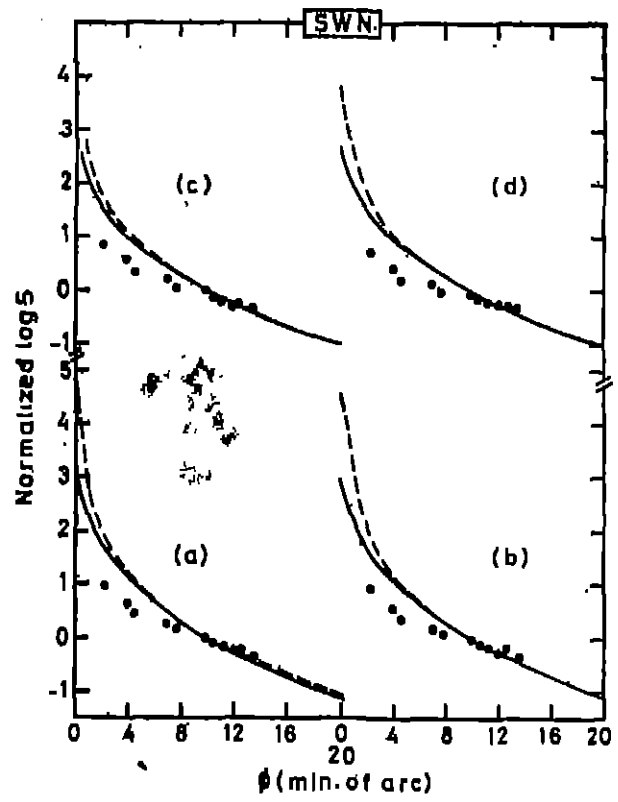

Fig. 3. The same as Figure 1, but for the case of the star within the nebula (SWN). The curves —.—.—.— for $a_o = 0.1$ μm and ..... for $a_o = 0.4$ μm represent a sample calculation for H=0.05 pc.

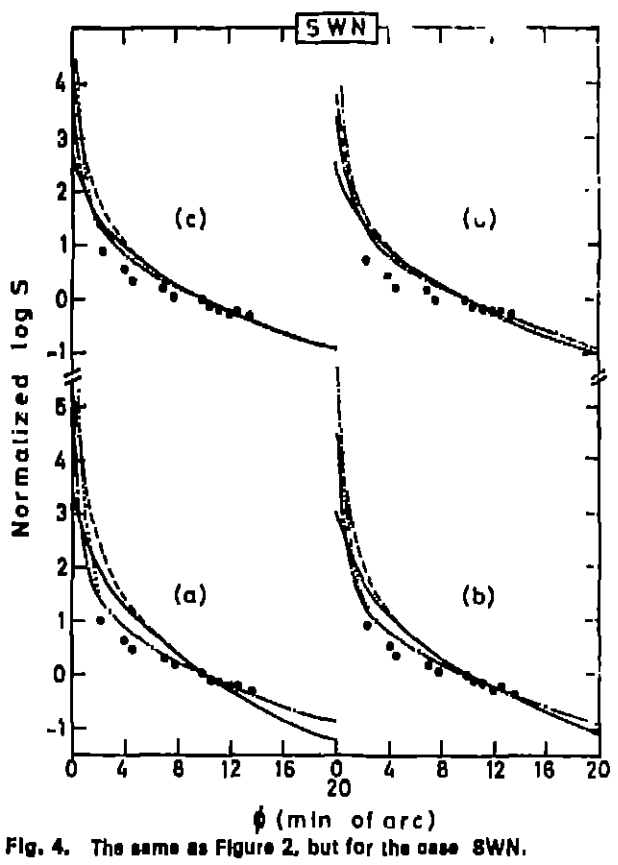

Fig. 4. The same as Figure 2, but for the case SWN.

nebula is normalized in such a manner that log S (λ, a_o, ϕ = 10′) = 0 for all wavelengths and size parameters. This scheme facilitates the comparison of model results with the observations reduced in a similar fashion. The sets (a), (b), (c) and (d) are plotted in each of these figures for wavelengths λ = 1650Å, 1800Å, 2200Å and 2500Å, respectively. The solid curves are for the size parameter a_o = 0.1 μm and the dashed curves are for a_o = 0.4 μm. The case of SWN for graphite as well as silicate grains, Figures 3 and 4, show the steepest gradients and largest span in the variation of the theoretical log S with respect to ϕ as compared to other two cases of SBN and SFN. These general trends are similar to those shown by ice grains in Paper I. For both graphite and silicate grains, the larger the size parameter a_o, the greater is the range in log S as one goes from ϕ = 0 to 20′. The effect of varying a_o from 0.1 μm to 0.4 μm is not noticeable in Figure 5 for graphite. The size effect of graphite grains is most pronounced in the geometric case SBN; SWN comes next and in case of SFN it is almost nil. Whereas for silicate grains, the order in which the size effect is important is seen to be SBN, SWN and SFN for ϕ equal to zero to ~8′, but beyond ϕ ~10′ the case of SWN shows very small change in log S compared to the SBN and SFN. The silicate grains can provide a close matching between the calculated and the observed surface brightness as indicated by Figure 6 for SFN. However, as remarked in Paper I, the case of SWN with the star very near to the front

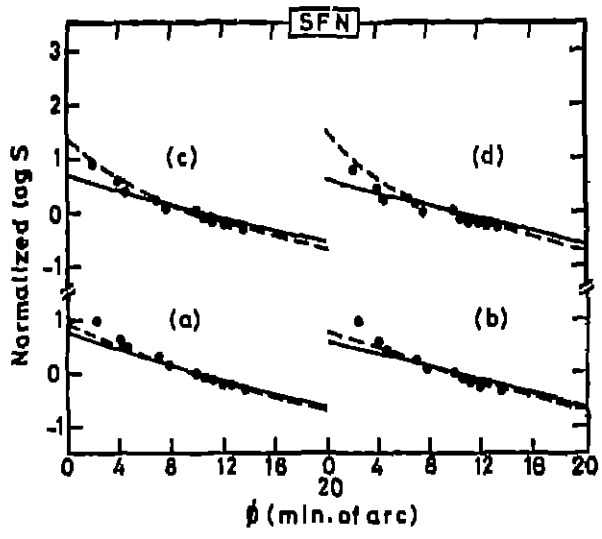

Fig. 5. The same as Figure 1, but for the case of the star in front of the nebula (SFN). Note that the curves for a_o=0.1 μm and 0.4 μm are almost identical.

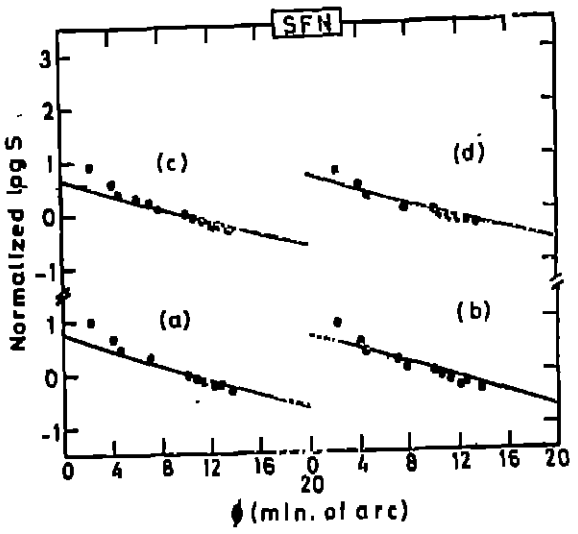

Fig. 6. The same as Figure 2, but for the case SFN

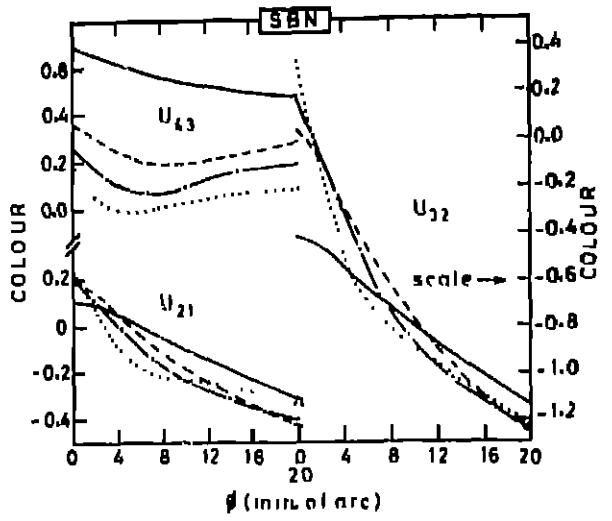

Fig. 7. The far-ultraviolet colour differences between two consecutive bands for the star minus the same for the reflection nebula. The geometrical case is SBN. The grains are composed of graphite with the size parameter a_0 = 0.1 μm for _____, 0.2 μm for – – – –, 0.3 μm for —·—·—·—, and 0.6 μm for

surface cannot be ruled out for silicate and/or ice grains. The improvement in matching is expected if one notices in Figure 3 that the reduction in H, the distance between the star and the front surface of the nebula, from 0.25 pc to 0.05 pc significantly brings the curves for a_0 = 0.4 μm near to the observational run for all the four wavelengths.

2.2 *Colours*

The star-minus-nebula colour differences expressed in magnitude and designated by U_{21}, U_{32} and U_{43} are defined by

$$U_{ji} = (U_j - U_i)_* - (U_j - U_i)_N$$

where j = 2, 3 or 4 corresponding to i = 1, 2 or 3 in respective order and * and N stand for star and nebula, respectively. The calculated colour differences are set out in Figures 7, 9 and 11 for graphite and in Figures 8, 10 and 12 for silicate. The general trends of blueing in the vicinity of the star and reddening relatively away from the star are noticeable for U_{21} in cases of SBN and SWN provided one chooses $0.1\,\mu m \lesssim a_0 \lesssim 0.4\,\mu m$ for graphite and $a_0 \sim 0.1$ μm for silicate grains. The U_{21} colours for silicate grains of size a_0 = 0.1 μm with SFN in Figure 12 also show positive colours in the neighbourhood of star and negative colours beyond $\phi \sim 10'$.

If there are graphite grains in the reflection nebula it should be possible to observe some correlating behaviour with respect to the hump at $\lambda = 2200$ Å in the general interstellar extinction curve

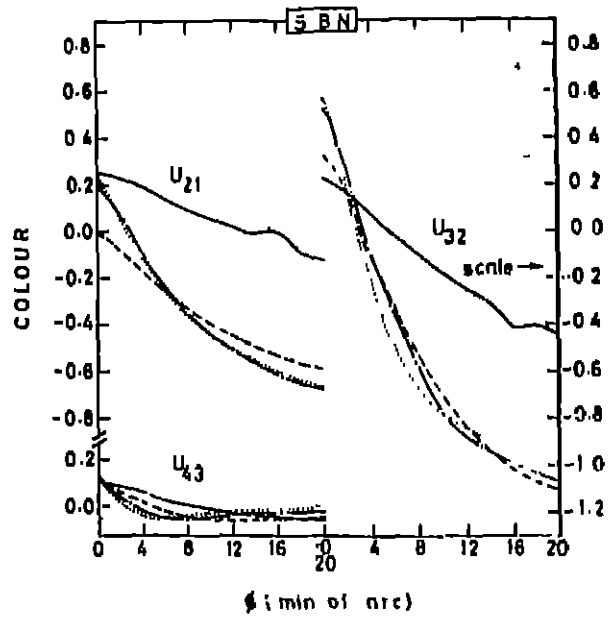

Fig. 8. The same as Figure 7 but with enstatite silicate grains having the size parameter a_0 = 0.1 μm for _____, 0.2 μm for – – – –, 0.3 μm for —·—·—·—, and 0.4 μm for .....

(see, for example, Bless and Savage, 1972; Nandy, Thompson, Jamar, Monfils and Wilson, 1975). However, all the bands selected in the far-ultraviolet observations have some overlap with the wavelength range $\lambda^{-1} \sim 4$ to 6 μm^{-1} where the extinction hump occurs. The detailed observations in the far-ultraviolet with and without inclusion of the hump wave-

length range would allow one to discriminate for or against graphite grains among various contending grain species.

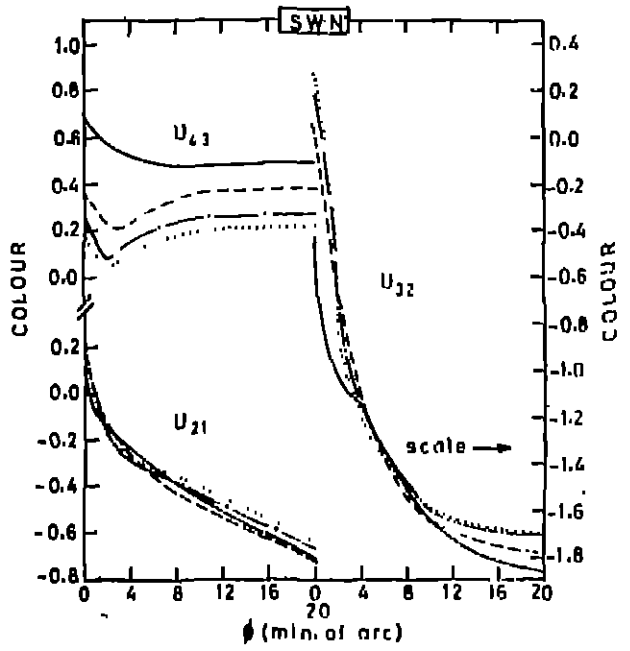

Fig. 9. The same as Figure 7, but for the geometrical case SWN and the size parameter as given in Figure 8.

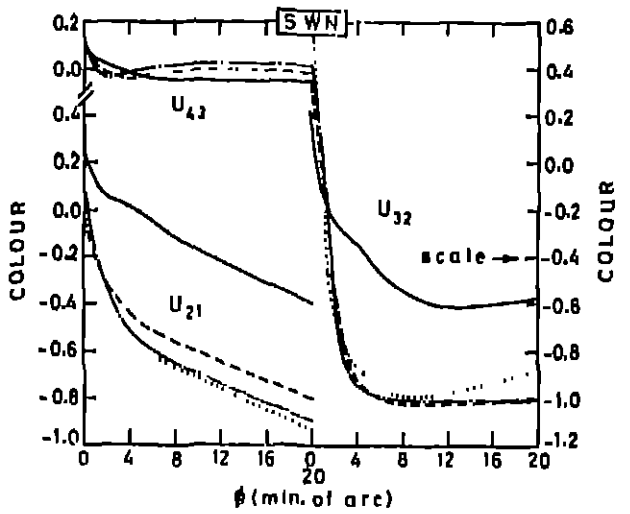

Fig. 10. The same as Figure 8, but for the geometrical case SWN.

The size effect is more pronounced for U_{43} with graphite and for U_{21} and U_{32} for silicate in all the three geometrical cases. However, they do not exhibit one-to-one correspondence with the variation of the surface brightness. The gradients of curves for U_{32} with silicate grains, especially when $a_0 = 0.2$, 0.3 and 0.4 μm, in the case of SFN in Figure 12 are

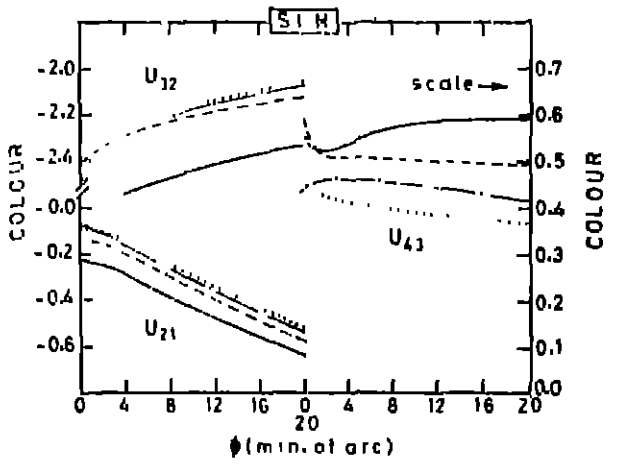

Fig. 11. The same as Figure 7, but for the geometrical case SIN and the size parameter as given in Figure 8.

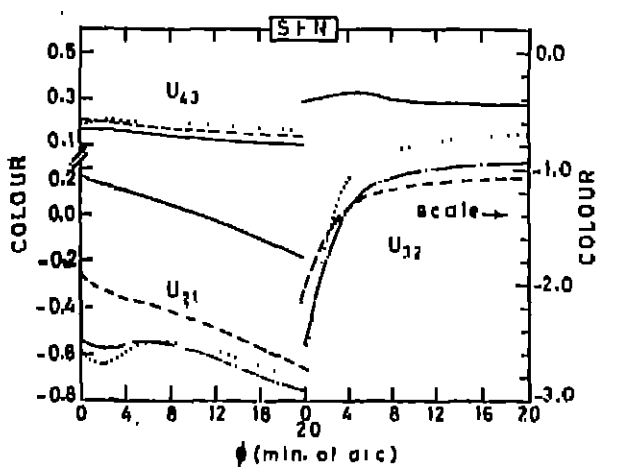

Fig. 12. The same as Figure 8, but for the geometrical case SFN.

in sharp contrast with the other geometrical configurations and also with the UBV photometric colour differences. The U_{43} colours appear monotonous except for graphite with SBN as well as SWN and $a_0 = 0.2$, 0.3 and 0.4 μm in Figures 7 and 9 and with SFN and $a_0 = 0.1$ μm and 0.3μm in Figure 11. The silicate grains in the case of SFN and $a_0 = 0.3$ and 0.4 μm also do not show monotonous variation in U_{21} colours in Figure 12. Note that the colour differences U_{21} for graphite in Figure 11 and U_{43} for silicate in Figure 12 both for 0.1 μm $\lesssim a_0 \lesssim$ 0.4 μm show nearly linear variation with ϕ from 0 to 20'. In general, the colours for various size parameters are more separated compared to the surface brightness for the same set of parameters.

2.3 *Polarization*

The theoretical results on the band integrated degree of polarization of nebular light for three

geometrical models SBN, SWN and SFN are plotted in Figures 13, 15 and 17 for graphite and in Figures 14, 16 and 18 for silicate grains. The sets (a), (b), (c) and (d) in each of these figures refer to far-ultraviolet bands U_1, U_2, U_3 and U_4, respectively. Although there are no observations on polarization available in the far-ultraviolet, one can get a rough idea of possible polarization on the basis of UBV photometry by Elvius and Hall (1966, 1967). These results as summarized by Shah (1977) indicate that the polarization is positive for all offset angles from $\phi = 0$ to $\phi = 18'$ and is of the order of $P_v \simeq 12\%$ and $P_b \simeq 8\%$ both for offset angle $\phi \simeq 20'$. Thus one may safely assume a few % polarisation in the far-ultraviolet U_1-band for large offset angle $\phi \simeq 20'$. An important question is whether one can have negative polarization in the far-ultraviolet. We would like to leave this question open. It may be noted that the wavelength dependence of polarization of Merope seem to be variable (Markkanen, 1977).

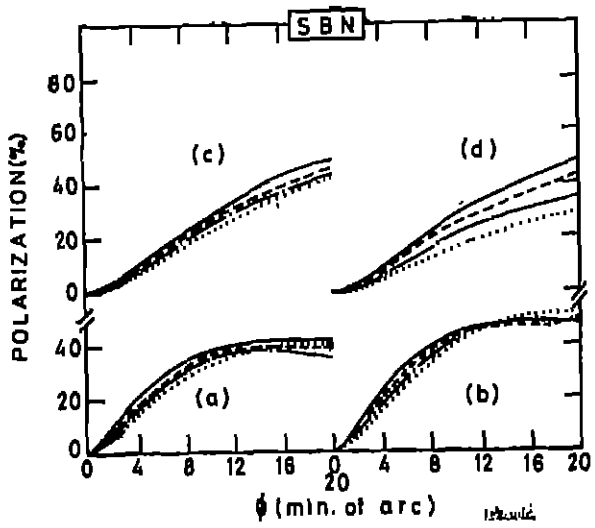

Fig. 13. The far-ultraviolet polarization produced by graphite grains in the model reflection nebula with the star in the rear (SBN). The sets (a), (b), (c) and (d) correspond to the ultraviolet bands U_1, U_2, U_3, and U_4, respectively. The size parameter $a_0 = 0.2\ \mu m$ for _____, $0.3\ \mu m$ for — — — —, $0.4\ \mu m$ for —.—.—.— and $0.6\ \mu m$ for .....

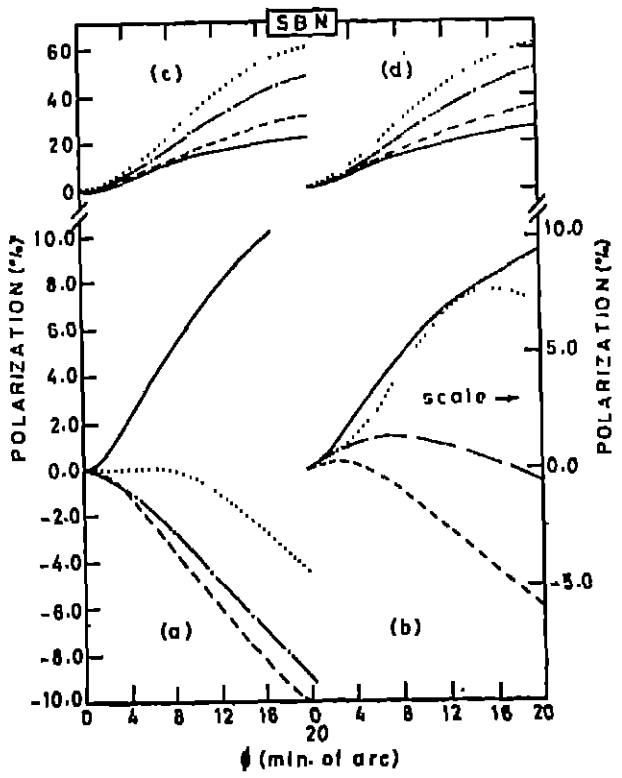

Fig. 14. The same as Figure 13 except that the grains are composed of enstatite silicate. The size parameter $a_0 = 0.1\ \mu m$ for _____, $0.2\ \mu m$ for — — — —, $0.3\ \mu m$ for —.—.—.— and $0.4\ \mu m$ for .....

On the basis of U_1-polarization alone one can eliminate the possibility of graphite grains as significant component in all the three geometrical cases of SBN, SWN and SFN because of the very large positive polarization for the chosen size parameters and $\phi = 20'$. Also, for graphite grains, P_{U2}, P_{U3} and P_{U4} give abnormally large values of polarization which are less likely to occur in the far-ultraviolet wavelength range beyond U_1. Note that the silicate grains in the case of SFN provide negative polariza-

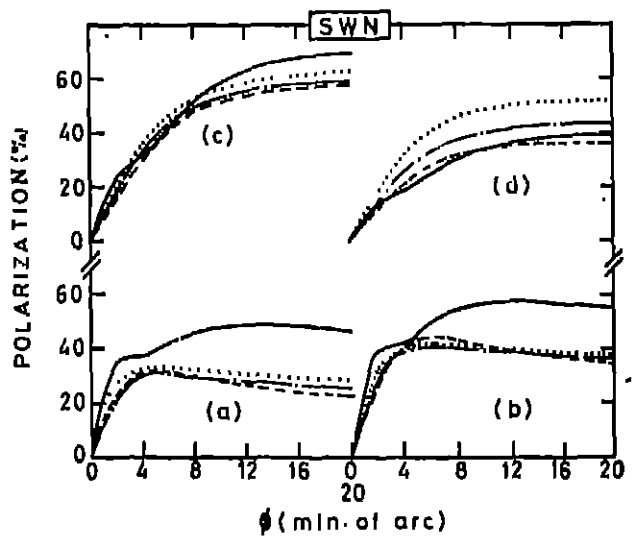

Fig. 15 The same as in Figure 13 except that the geometrical case is SWN and that the size parameter a_0 is as given in Figure 14.

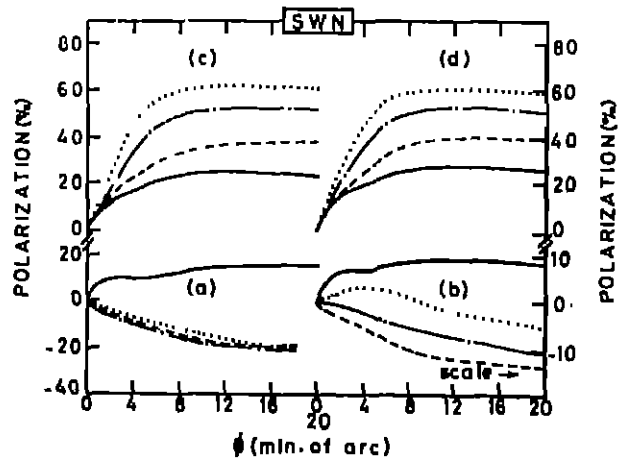

Fig. 16 The same as Figure 14 but the geometrical case is SWN.

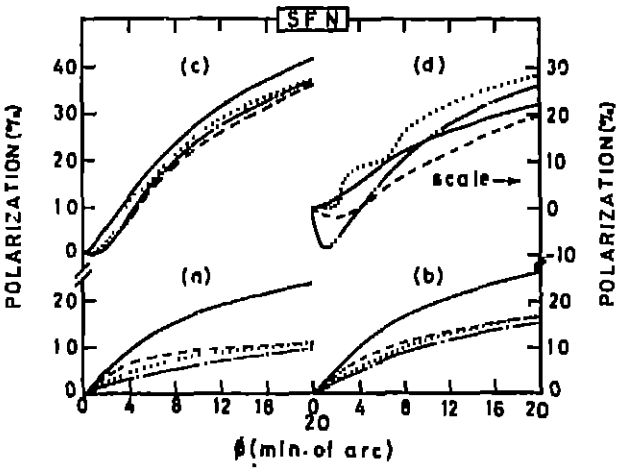

Fig. 17. The same as Figure 13 except that the geometrical case is SFN and that the size parameter a_0 is as given in Figure 14.

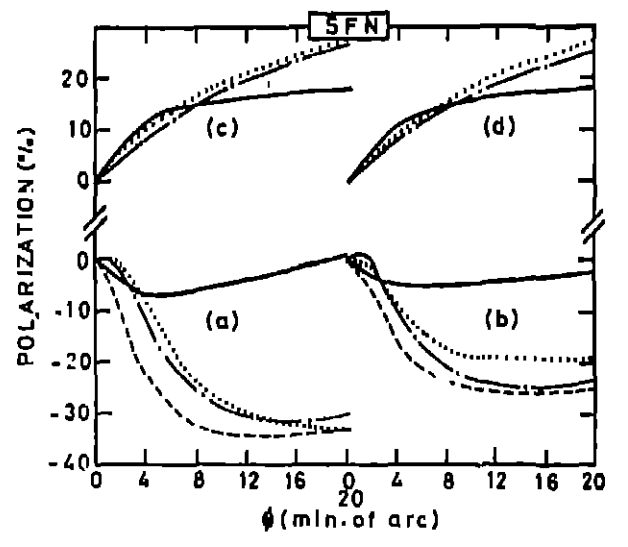

Fig. 18. The same as Figure 17, but the grains are composed of enstatite silicate.

tion in the U_1-band for $a_0 = 0.1$ (0.1) 0.4 μm and for all offset angles. A small positive polarization in U_1-band can be satisfied by silicate grains with $a_0 \sim 0.1$ μm in combination with $a_0 \sim 0.2$ μm provided one adopts either SBN or SWN.

3. Conclusion

In view of the present results and Paper I, it may be concluded that the ice and silicate grains are likely to be important constituents of the interstellar grains in the Merope reflection nebulosity. Regarding the position of the star relative to the nebula we need to study further with additional observational data to pinpoint the correct geometrical configuration of the nebula. As suggested by Jura (1977) future observations of rotationally excited molecular hydrogen can help in determining whether the dust that produces the reflection nebulosity is in front of or behind the star Merope (23 Tau). The observations of infrared radiation in coordination with the visual and ultraviolet observations may be used for discriminating among the various proposed compositions of the interstellar grains. This may also allow one to choose appropriate model of the star-nebula configuration.

Either multidimensional size distributions of the grains and/or core-mantle grains within the nebula are worth considering when detailed observations on the colours and polarizations in the infrared, visual and far-ultraviolet wavelength ranges are available. Extremely fine filamentary structure of the Merope nebula (see, for example, Elvius and Hall, 1966, 1967 : Arny, 1977 ; and Markkanen, 1977) hints at the existence of significant magnetic fields within the nebula. Therefore, the role of magnetic orientation of the non-spherical particles must be examined in future models of the Merope reflection nebula.

Acknowledgement

One of us (G.A.S) would like to thank Dr. M. K. V. Bappu for encouragement in this work.

References

Andriesse, C. D., Piersma, Th. R., Witt, A. N., 1977, *Astr. Astrophys.*, **54**, 841
Arny, T., 1977, *Astrophys. J.*, **217**, 83
Bless, R. C., Savage, B. D., 1972 *Astrophys. J.*, **171**, 293.,

Elvius, A., Hall J. S., 1966, *Lowell Obs. Bull.*, 6, 257.
Elvius, A., Hall, J. S., 1967, *Lowell Obs. Bull.*, 7, 17.
Huffman, D. R., Stapp, J. L., 1971, *Nature Phys. Sci.*, 229, 46.
Jura, M., 1977, *Astrophys. J.*, 216, 749.
Markkanen, T., 1977, *Astron. Astrophys.*, 58, 83.
Nandy, K., Thompson, G. I., Jamar, C., Monfils, A., Wilson, R 1975, *Astr. Astrophys.*, 44, 195.
Philipp, H. R., Taft, E. A., 1962, *Phys. Rev.*, 127, 159.
Shah, G. A., 1977, Pramana, 9, 461.
Shah, G. A., Krishna Swamy, K. S., 1978, *Kodaikanal Obs. Bul. Ser. A.*, 2, 95.